Extracellular Vesicle-Educated Macrophages Promote Early Achilles Tendon Healing

CONNIE S. CHAMBERLAIN [ORCID],[a] ANNA E. B. CLEMENTS,[a] JOHN A. KINK,[b,c] UGEUN CHOI,[a,d]
GEOFFREY S. BAER,[a] MATTHEW A. HALANSKI,[a] PEIMAN HEMATTI,[b,c] RAY VANDERBY[a,d]

Key Words. Macrophages • Mesenchymal stromal cells • Achilles tendon injury •
Extracellular vesicles • Tendon healing

aDepartment of Orthopedics
and Rehabilitation, University
of Wisconsin, Madison,
Wisconsin, USA; bDepartment
of Medicine, University of
Wisconsin, Madison,
Wisconsin, USA; cUniversity of
Wisconsin Carbone Cancer
Center, University of
Wisconsin, Madison,
Wisconsin, USA; dDepartment
of Biomedical Engineering,
University of Wisconsin,
Madison, Wisconsin, USA

Correspondence: Ray Vanderby,
Ph.D., Department of
Orthopedics and Rehabilitation,
1111 Highland Ave., 5059 WIMR,
University of Wisconsin-Madison,
Madison, Wisconsin 53705, USA.
Telephone: 608-263-9593;
e-mail: vanderby@ortho.wisc.edu;
or Peiman Hematti, M.D.,
Department of Medicine, 1111
Highland Ave., 4033 WIMR,
University of Wisconsin-Madison,
Madison, Wisconsin 53705, USA.
Telephone: 608-265-0106;
e-mail: pxh@medicine.wisc.edu

Received April 5, 2018; accepted
for publication January 21, 2019;
first published online in STEM
CELLS EXPRESS February 5, 2019.

http://dx.doi.org/
10.1002/stem.2988

ABSTRACT

Tendon healing follows a complex series of coordinated events, which ultimately produces a mechanically inferior tissue more scar-like than native tendon. More regenerative healing occurs when anti-inflammatory M2 macrophages play a more dominant role. Mesenchymal stromal/stem cells (MSCs) are able to polarize macrophages to an M2 immunophenotype via paracrine mechanisms. We previously reported that coculture of CD14+ macrophages (MQs) with MSCs resulted in a unique M2-like macrophage. More recently, we generated M2-like macrophages using only extracellular vesicles (EVs) isolated from MSCs creating "EV-educated macrophages" (also called exosome-educated macrophages [EEMs]), thereby foregoing direct use of MSCs. For the current study, we hypothesized that cell therapy with EEMs would improve in vivo tendon healing by modulating tissue inflammation and endogenous macrophage immunophenotypes. We evaluated effects of EEMs using a mouse Achilles tendon rupture model and compared results to normal tendon healing (without any biologic intervention), MSCs, MQs, or EVs. We found that exogenous administration of EEMs directly into the wound promoted a healing response that was significantly more functional and more regenerative. Injured tendons treated with exogenous EEMs exhibited (a) improved mechanical properties, (b) reduced inflammation, and (c) earlier angiogenesis. Treatment with MSC-derived EVs alone were less effective functionally but stimulated a biological response as evidenced by an increased number of endothelial cells and decreased M1/M2 ratio. Because of their regenerative and immunomodulatory effects, EEM treatment could provide a novel strategy to promote wound healing in this and various other musculoskeletal injuries or pathologies where inflammation and inadequate healing is problematic. STEM CELLS 2019;37:652–662

SIGNIFICANCE STATEMENT

Tendon healing results in a mechanically inferior tissue more scar-like than native tendon. To improve healing outcome, M2-like macrophages were generated by exposing CD14+ macrophages to extracellular vesicles (EVs), creating "EV-educated macrophages" (exosome-educated macrophages [EEMs]). EEM treatment to a tendon injury accelerated biological and functional healing. These results have significant clinical relevance in that (a) EEMs are terminally differentiated and will not proliferate or differentiate into undesirable cell types in vivo, (b) EEMs can be generated using off-the-shelf EVs, and monocytes collected from a patient's own blood, and (c) the immune-modulatory effects of EEMs suggest this approach may benefit other inflammatory conditions.

INTRODUCTION

Tendon healing involves a complex, coordinated series of events that fails to regenerate the composition and mechanical properties of native tissue. Despite new surgical techniques and other therapies designed to improve healing and/or minimize scar formation, the quality and speed of repair remain problematic. Macrophages are emerging as key players in tissue homeostasis and the tendon repair process. Macrophages can be categorized into two broad subsets including the M1 (classically activated) and the M2 (alternatively activated) macrophages. Although the M1 and M2 (further subdivided into M2a, M2b, M2c, and M2d macrophages) dichotomy is insufficient to encompass all of their diverse phenotypes and functions, the M1 macrophages, in general, appear first to mediate tissue damage, support pathogen killing and are pro-inflammatory. The M2 macrophages are responsible for limiting the area of tissue damage, antagonizing the M1 macrophage response, reducing inflammation, and promoting tissue repair [1–3].

Numerous studies have demonstrated the significance of macrophages during wound repair and their involvement in regeneration. For example, the axolotl has the remarkable ability to regenerate complex structures such as the limbs, tails, and spinal cord. Within the regenerating axolotl limb, M2-associated anti-inflammatory cytokines, which are normally induced later in mammalian wound healing, were detected within 1 day of axolotl limb resection [4]. In chronic inflammatory models, including chronic venous ulcers, obesity associated inflammation, and atherosclerosis, macrophages fail to switch from an M1 to an M2 phenotype and healing is delayed [5–7].

Macrophage polarization, both in vitro and in vivo, can be induced by mesenchymal stromal/stem cell (MSC) paracrine activity [8–17]. In mammalian models of ligament or tendon healing, MSC treatments increased the presence of endogenous M2 macrophages and associated anti-inflammatory cytokines, which subsequently resulted in improved tendon and ligament healing [18–22]. We previously reported that MSCs uniquely educate macrophages toward an anti-inflammatory phenotype (MSC-educated macrophages [MEMs]) [23]. Compared with steady state control macrophages (MQs), MEMs exhibited a unique phenotype in which high levels of IL-10 and IL-6 and low level of IL-12 and TNF-α were expressed. In mouse models, MEMs enhanced mouse survival during lethal graft-versus-host disease and after radiation injury when compared with MSCs or macrophage treatments [24]. MSCs secrete many growth factors and cytokines to modulate healing, but we hypothesized that an important paracrine signaling mechanism to affect macrophage phenotype and healing is via extracellular vesicles (EVs). EVs are small (40–200 nm) lipid membrane vesicles formed by inward budding of late endosomes and released into the extracellular environment upon fusion with the cell plasma membrane of the donor cell. Although EVs are constitutively secreted by many cell types, their bioactive molecules and subsequent intercellular signaling are cell-specific and play key roles in intercellular communication [25, 26]. In this study, we tested the use of MSC-derived EVs/exosomes to educate macrophages, to create an M2-like phenotype (exosome-educated macrophages [EEMs]), and to influence tendon healing. We hypothesized that the application of exogenous human MSC-derived EV-educated macrophages improves tendon healing by modulating tissue inflammation and endogenous macrophage immunophenotypes.

MATERIALS AND METHODS

Cell Culture

All protocols were approved by the Health Sciences Institutional Review Board of University of Wisconsin-Madison, School of Medicine and Public Health. Monocytes were isolated from human peripheral blood using magnetic bead separation methods according to manufacturers' protocols. Briefly, peripheral blood mononuclear cells were collected from the discarded left-overs of Granulocyte-colony stimulating factor(G-CSF) mobilized peripheral blood of healthy donors by density gradient separation using Ficol-Paque Plus 1.073 (GE Healthcare Bio-Sciences, Piscataway, NJ). Residual red blood cells were lysed by incubating cells in Ammonium-Chloride-Potassium (ACK) lysis buffer for 3–5 minutes and mononuclear cells were washed with phosphate-buffered saline (PBS). To reduce platelet contamination, cell suspensions were centrifuged at 300–700 rpm for 10 minutes and cell pellets

were resuspended and incubated with anti-human CD14 microbeads (Miltenyi Biotech, Auburn, CA) for 15 minutes at 4°C. After washing to remove unbound antibody, cell separation was accomplished using an autoMACS Pro Separator (Miltenyi Biotech). Purity of the isolated CD14+ cells was >95% when checked with flow cytometry. Purified CD14+ monocytes were either plated into six-well culture plates at a concentration of 0.5–1 × 10^6 per well or 10^7 per T75 cm^2 filter cap cell culture flask (Greiner Bio-One, Monroe, NC) in Iscove's modified Dulbecco's media supplemented with 10% human serum blood type AB (Mediatech, Herndon, VA), 1× nonessential amino acids (Lonza, Walkersville, MD), 4 mM L-glutamine (Invitrogen, Carlsbad, CA), 1 mM sodium pyruvate (Mediatech), and 4 μg/ml recombinant human insulin (Invitrogen). Cells were cultured for 7 days at 37°C with 5% CO_2, without adding any cytokines, to differentiate to macrophages. Attached cells were harvested using Accumax dissociation media (Innovative Cell Technologies, Inc., San Diego, CA) followed by using a cell-scraper.

MSCs were isolated from filters left over after bone marrow (BM) harvest from normal healthy donors [27]. Briefly, BM cells trapped in the filter were recovered by rinsing the filter with PBS, and mononuclear cells were separated using Ficol-Paque Plus 1.073 (GE Health Care Bio-Sciences). Red blood cells were lysed with 3–5 minutes incubation in ACK lysis buffer and mononuclear cells were suspended in α-minimum essential medium supplemented with 10% fetal bovine serum (U.S. Origin, uncharacterized; Hyclone, Logan, UT), 1× nonessential amino acids, and 4 mM L-glutamine. Cells were cultivated in 75-cm^2 filter cap cell culture flasks. Attached cells (passage 0) were harvested using TrypLE cell dissociation enzyme (Invitrogen) and then replated into new flasks as described previously [23, 24]. Passage 4–6 cells were confirmed to be MSC's processing the typical marker profile by flow cytometry [28] and the MSC cultures were used for isolation of EVs.

Isolation and Characterization of EVs from MSCs

MSCs grown to confluence in 75-cm^2 filter cap cell culture flasks were washed once with PBS, and the media was replaced with StemPro MSC serum-free media CTS (Gibco Life Technologies, Gaithersburg, MD). Cells were incubated for 18–24 hours and the conditioned culture media (CM) was collected and EVs were isolated by differential ultracentrifugation essentially as previously described [29]. The CM was centrifuged using a Beckman Coulter Allegra X-15R centrifuge at 2,000g at 4°C for 20 minutes to remove any detached cells, apoptotic bodies and cell debris. Clarified supernatant CM was then centrifuged in a Beckman Coulter Optima L-80XP Ultracentrifuge at 100,000g at 4°C for 2 hours with a swinging bucket SW 28 rotor to pellet EVs. The supernatant was carefully removed, and EV-containing pellets were resuspended PBS and pooled. The EV pellet was suspended at 100 μl PBS/10 ml of conditioned media and characterized using a Thermo Nano-Drop spectrophotometer for protein and RNA concentration. Particle diameter and concentration were assessed using an IZON qNano Nanoparticle Characterization instrument (Zen-bio, Inc., Research Triangle Park, NC).

MACSPlex Flow Cytometry of EVs

The characterization of surface markers present in the MSC EVs was performed by Zen-Bio, Inc. by flow cytometry using the MACSPlex Exosome Kit (Miltenyi Biotec). This kit allows for the detection of up to 37 known exosomal surface markers
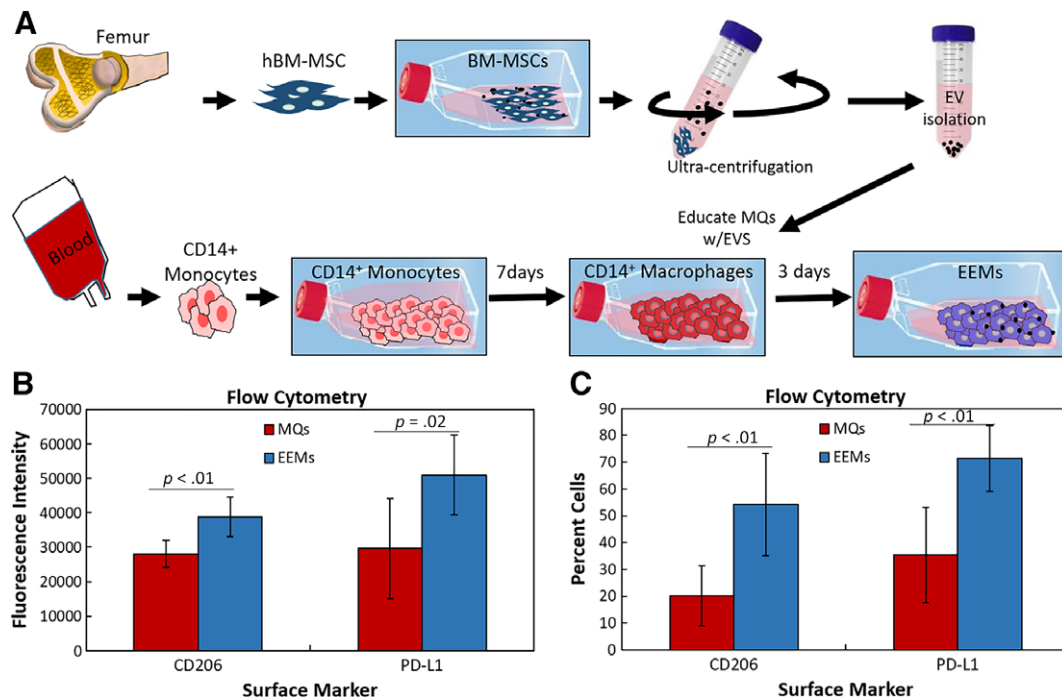
Figure 1. Fabrication and characterization of exosome-educated macrophages (EEMs). **(A):** Bone marrow mesenchymal stromal/stem cells (MSCs) were culture expanded. Extracellular vesicles (EVs) were then isolated from the MSCs via ultracentrifugation. CD14+ monocytes were obtained from human peripheral blood. Monocytes were cultured for 7 days, activated to CD14+ macrophages, and then educated with EVs for 3 days, producing EEMs. **(B, C):** CD14+ macrophages (control macrophages [MQs]) and EEMs were measured for alternatively activated macrophage cell surface markers by flow cytometry. (B): Fluorescence intensity and (C) percent cells indicate more EEMs were positive for CD206, and PD-L1 compared with the MQs. *, p values are results of Fisher's least significant difference (LSD) post hoc pairwise analysis ($p < .05$). Values are expressed as mean cell numbers $\pm$ SD.

plus two isotype groups which served as background controls. The assay was performed according to manufacturer's protocol. In brief, capture beads coupled with antibodies to the EV surface markers were mixed with equal volumes of purified MSC EVs and gently rotated in the dark at 4°C overnight. The bead-EV complexes were washed and incubated for 1 hour with detection bead mixture consisting of pan-EV markers CD9, CD63, and CD81 labeled with Fluorescein isothiocyanate (FITC), phycoerythrin (PE), or allophycocyanin (APC). The beads were then washed and resuspended in MACSPlex buffer for analysis. Prior to experimentation, the system was calibrated and background settings were adjusted to unlabeled beads. The autosampler used 100 μl from each sample to collect beads and automated gating strategies were used to identify bead populations for each analyte. Batch analysis quantified median intensities for each bead population and analyte surface expression was calculated for each sample. Miltenyi MACSQuant Analyzer 10 for sample acquisition and MACSQuantify Software were used for data analysis. Median fluorescent values of 1.0 or more were considered positive for the marker and means were determined from EVs isolated from different MSC isolates.

Education of Macrophages to M2 Phenotype Using EVs from MSCs

Macrophages were "educated" by EVs isolated from the MSCs (Fig. 1A). EVs were added to macrophages on day 7 and then cultivated for 3 more days to generate EEMs in 75-cm² filter cap cell culture flasks (10 ml) using approximately 3×10^9 EVs per flask of cells. MQs controls were treated with PBS. The macrophages were harvested by removing media, washing with PBS

then using Accumax cell dissociation enzyme (Innovative Cell Technologies) to detach the cells from the flask followed by the use of a cell scraper. A sample of the MQs and EEMs were analyzed by flow cytometry, and the remainders were used in the animal studies. The cells used for animal studies (MQs, EEMs, as well as MSCs) were then labeled with Cell Tracker CM DiI (Invitrogen, Eugene, OR) to allow in vivo tracking.

Flow Cytometry of EEMs

MQs or EEMs at day 10 of culture were collected, counted and incubated with Fc block (BD Pharmingen, San Jose, CA) and stained for surface markers at 4°C for 20–30 minutes with anti-human antibodies including PerCP/Cy5.5-CD14 (HCD14), PE-CD206 (15-2S), and APC-PD-L1 (29E.2A3). All antibodies were purchased from BioLegend (San Diego, CA). Compensation was achieved using Ultra-comp beads (catalog no. 01-2222-42, E-bioscience). Flow cytometry data were acquired on an Acuri C9 cell analyzer (BD Biosciences, San Jose, CA). CD14+ cells were evaluated for the presence of CD206 and PD-L1 markers by determining the median fluorescence intensity of the cells and percent cells stained.

Achilles Tendon Healing Model

All procedures were approved by the University of Wisconsin-Madison Institutional Animal Care and Use Committee. All surgeries were performed using isoflurane for anesthesia. All efforts were made to minimize suffering. Twenty-seven skeletally mature male nude (*Foxn1nu*) mice (9–10 weeks old) were used as an animal model to study normal Achilles tendon healing after unilateral surgical transection. A surgically transected

rather than torn tendon was used as an experimental model to create a uniform defect to compare healing. A skin incision was made, subcutaneous layer and muscle dissected, and the underlying Achilles tendon and superficial digital flexor (SDF) tendon were exposed on the right hind limb. The SDF was separated from the Achilles tendon and removed. The Achilles tendon was then completely transected at the midpoint (half way between the calcaneal insertion and the musculotendinous junction; determined using a scaled scalpel handle). Tendon ends were sutured together using 5-0 Vicryl suture. A surgical pouch using the muscular layer was then constructed over the tendon injury. Treatments (20 µl) were administered within the pouch directly over the surgically repaired Achilles tendon and the pouch was closed by suturing. Treatments to the injured Achilles tendon included (a) Hank's balanced saline solution (serving as the injured control), (b) 1×10^6 human BM-MSCs, (c) 1×10^6 CD14$^+$ MQs, or (d) 1×10^6 EEMs. The use of human BM MSCs serves as a comparative cellular treatment that is receiving extensive interest as a tendon healing therapy. The left Achilles tendon remained intact and served as a contralateral control.

Following transection and repair of Achilles tendon, the joint was immobilized using a wire cerclage. Immobilization of the hock is critical to preserve the suture repair of the Achilles tendon and in our experience, Achilles tendons without hock immobilization frequently result in suture failure and tendon rerupture. To account for potential stress shielding effects by the immobilization process, the injured only group was also subjected to hock immobilization. For this procedure, a hole was drilled in the tuber calcaneus. Surgical steel suture was passed proximally, through the fibular-tibial fork, and distally through the hole in tuber calcaneus. The wire ends were twisted together and tightened, placing the hock in full plantar flexion. The skin was sutured closed after insertion of the cerclage and repair of the Achilles.

Tendons were collected at days 7 and 14 and used for mechanical testing or immunohistochemistry (IHC) or histology. Days 7 and 14 were chosen to study treatment effects on early tendon healing with specific focus on endogenous macrophages, which are peaking in number at 7 days after injury. Day 14 was chosen to measure angiogenesis as well as early extracellular matrix (ECM) formation. Day 14 was also chosen as a time that the tendon would be healed sufficiently to assay early tissue function via mechanical testing. Tendons used for IHC were carefully dissected and immediately embedded longitudinal/frontal, in optimal cutting temperature medium for flash freezing. Animals used for mechanical testing were sacrificed and limbs were stored in toto at -70°C until processed. Mechanical testing was not performed on day 7 because tendons were too structurally compromised for meaningful functional data. Based on preliminary results indicating a healing tissue effect, an additional treatment group of EVs alone was included. The amount of EVs administered to each animal equaled the amount of EVs used to educate macrophages. Tissue was collected 14 days after injury and measured for mechanical testing and IHC. Based on equivocal results at day 14, a day 7 after injury group was not included in the study.

IHC/Immunofluorescence/Histology

In order to identify cellular and ECM changes within the healing tendon after treatment, IHC, immunofluorescence (IF) and histology were performed on days 7 and 14 Achilles tendons.

Longitudinal cryosections were cut at a 5 µm thickness, mounted on Colorfrost Plus microscope slides and maintained at -70°C. IF and IHC was performed on frozen sections. In order to visualize implanted DiI positive cells within the healing tendon, cryosections were placed on slides, fixed in acetone, washed in PBS, and coverslipped using Prolong Gold Anti-fade Reagent containing DAPI (Invitrogen). For IHC, cryosections were fixed in acetone, exposed to 3% hydrogen peroxide to eliminate endogenous peroxidase activity, blocked with Rodent Block M (Biocare Medical, Pacheco, CA) and incubated with rabbit or rat primary antibodies. Primary rat monoclonal antibodies specific to mouse F4/80, CD206, CD31 (all 1:100, BioRad, Hercules, CA) were used to detect total macrophages, M2 macrophages, and endothelial cells, respectively. Rabbit polyclonal antibodies were used for type I collagen (1:800, Abcam-Serotec, Raleigh, NC) and type III collagen (1:150, Abcam-Serotec). Lastly, rabbit monoclonal CCR7 was used to identify M1 macrophages (1:1,200, Abcam-Serotec). After primary antibody incubation, samples were exposed to Rabbit or Rat HRP Polymer (Biocare Medical). The bound antibody complex was visualized using diaminobenzidine. Stained sections were dehydrated, cleared, cover-slipped and viewed using light microscopy. After IHC staining, micrographs were collected using a camera-assisted microscope (Nikon Eclipse microscope, model E6000 with an Olympus camera, model DP79). Approximately four tendon sections were captured and counted per animal. If tendon sections exhibited any processing flaws (not faced, wrinkled, torn, etc.) sections were omitted from further analyses. Images captured for measurement of total macrophages, M1 and M2 macrophages, endothelial cells, type I collagen, and type III collagen were quantified via Image J (National Institutes of Health, Bethesda, MD). Measurements were collected (a) within the granulation tissue and (b) within the entire section. Tendons stained for DAPI and DiI were analyzed for any presence of implanted cells at 7 or 14 days after injury. Tendon cryosections were also H&E stained to observe histological morphology of the healing tendon.

Fractal Analysis

Tissue organization was quantified by fractal dimension [30–32]. Fractal analysis is a useful quantitative method to evaluate collagen matrix organization and thereby providing a metric to rate healing and scar formation [32]. Tissue sections were H&E stained and images were captured. H&E images were cropped 4.5 in. × 4.5 in. to include the transected region. Images were converted from gray-scale to binary images using a threshold value that was automatically determined using the automatic gray-thresh command in MATLAB (Mathworks, Natick, MA). To improve contrast, the image was divided into 32 regions and the threshold for each region was determined separately. The sections were reaggregated to form a black and white image of the original version. Fractal analysis of each binary image was performed using a MATLAB routine, which calculated the fractal dimension using the Minkowski–Bouligand dimension (i.e., box counting dimension) [33]. The box counting dimension was determined by overlaying the image in successively smaller grids of boxes then counting the number of boxes required to cover the image. The number of boxes was plotted as a function of box size and the slope of the line computed. Fractal dimension was calculated as the average slope value for the three smallest box sizes. Fractal values range from 1 to 2 with a smaller fractal dimension indicating more linearly organized tissue.

Mechanical Testing

In order to test the mechanical properties of the healing tendon after macrophage treatment, only day 14 tendons were tested. Achilles tendons were dissected and surrounding tissue excised with care to keep the calcaneal insertion site intact. Tendons remained hydrated using PBS. Tendon length, width, and thickness were measured using a dissecting microscope and digital calipers at preload. Width and thickness measurements were obtained at the injury site. The cross-sectional area (assumed to be an ellipse) was then estimated. Tendons were tested in a custom-designed load frame, which gripped and loaded the tendons along their longitudinal axis. The calcaneus was trimmed and press-fit into a custom bone grip. The soft tissue end of the specimens was fixed to strips of Tyvek (McMaster-Carr, Elmhurst, IL) with adhesive (super glue; Ace Hardware Corporation, Oak Brook, IL), which were held between two plates forming the soft-tissue grip. Dimensional measurements for the tendons were recorded at preload. Mechanical testing was performed at room temperature. A low preload of 0.1 N was applied in order to obtain a uniform zero point [14] prior to preconditioning (20 cycles at 0.5 Hz) to 0.5%. Pull-to-failure testing was performed on tendons at a rate of 3.33 mm/second. Force and displacement data from the test system were recorded at 10 Hz. Failure force was the highest load prior to failure of the tendon and Lagrangian stress was calculated by dividing the failure force by the initial cross-sectional area. Stiffness was calculated by determining the slope of the linear portion of the load–displacement curve. Young's modulus was calculated by the slope of the linear portion of the stress–strain curve.

Statistical Analysis

A one-way analysis of variance (ANOVA) was used to examine treatment differences for the IHC and mechanical data. For each IHC procedure, results for each tissue section per animal (approximately four tissue sections) were averaged. The average of each animal/treatment was then subjected to ANOVA. If the overall p-value for the F-test in ANOVA was significant, post hoc comparisons were performed using the Fisher's LSD method. Experimental data are presented as the means $\pm$ SD. All p-values reported are two-sided. $p < .05$ was the criterion for statistical significance. Computations and figures were performed using KaleidaGraph, version 4.03 (Synergy Software, Inc., Reading, PA).

RESULTS

EV Measurements

The EVs from the human BM MSCs were characterized to determine mean particle size and concentration using either the IZON qNano particle characterization system or a Nanosight NS300 instrument. Mean particle size was found to be 61–121 nM in size with a particle concentration of 1–6×10^{11} particles per milliliter. Based on particle size, the vast majority of EV preparation consisted of EV-sized vesicles. MACSPlex flow cytometry identified six known EV surface markers (Supporting Information Fig. S1), including CD146, CD29, CD44, CD63, CD81, and CD105. These markers are broadly involved in cell adhesion (CD146), receptor function (CD29, CD44), protein anchoring (CD63, CD81), and glycosylation (CD105).

EV Flow Cytometry

To characterize the immune-phenotype of EEMs compared with MQs, we examined the expression of CD206 and PD-L1 of the two biologic CD14+ macrophage isolates used in this study. CD206, a mannose receptor, is a well-known marker of M2 macrophages and our previously described MSC educated macrophages (MEMs); PD-L1 an immune-inhibitory checkpoint molecule [34, 35]. As shown in Figure 1B, 1C, CD206 and PD-L1 were significantly higher in mean fluorescence intensity and percent cells from EEMs compared with the control MQs, indicating the MSC-derived EVs were able to "educate" the macrophages to become more M2-like.

Mechanical Testing

To determine if our EEM treatment affected tendon function, the day 14 tendons (Fig. 2) were mechanically tested. Tendon failure load, ultimate stress, stiffness, and Young's modulus, were measured. Compared with all other groups, EEM treatment significantly increased ultimate stress ($p < .01$; Fig. 2A) and Young's modulus ($p = .03$; Fig. 2B). No significant difference was found in failure load ($p = .260$; Fig. 2C) and stiffness ($p = .30$; Fig. 2D). Altogether, these results support our hypothesis and indicate that EEM treatment substantially improves the mechanical properties of the healing tendon, even greater than MSC treatments.

IHC of Cellular Factors

IF was first performed to determine if cell treatments remained localized to the healing tendon after 7 and 14 days after injury. DiI labeled cells from all cell treatments (MSC, MQ, and EEM) were found localized within in the injured tendon 7 days after injury (Supporting Information Fig. S2). A few implanted MSCs and MQs were still apparent 14 days after injury, but no EEMs were evident. IHC was performed to determine if exogenous administration of EEMs modulate the endogenous inflammatory cell profile. Total macrophages were not significantly different between treatment groups at day 7 ($p = .97$) or 14 ($p = .25$). Furthermore, analysis of the macrophage immunophenotypes indicated that the number of day 7 endogenous M2 macrophages was significantly increased after either MQ ($p = .004$) or EEM treatment compared with injury and to MSC treatments (Fig. 3A, 3E–3I). Interestingly, M2 macrophages within the MSC treated group were similar in number to the injury only group. By day 14, no treatment effects were evident except that the number of M2 macrophages regardless of treatment, was reduced compared with day 7. M1 macrophages within the granulation tissue were not significantly different between treatment groups at day 7. However, by day 14 EEM treatment significantly reduced the number of M1s (Fig. 3B, 3J–3N). Additional examination of the macrophages indicated a significant decrease in the M1/M2 ratio within the day 14 tendons after EEM treatment (Fig. 3C). Lastly, EEM treatments also increased the number of day 7 endothelial cells ($p < .01$; Fig. 3D, 3O–3S), but no changes were noted by day 14.

Collagen Production and Organization

To examine the effects of EEM treatments on ECM repair and scar formation, fractal analysis quantified collagen organization, and IHC assays probed collagen production. Interestingly, type I collagen content was significantly reduced by both macrophage and EEM treatments. This reduction was noted specifically within the granulation tissue ($p = .05$) 7 days after
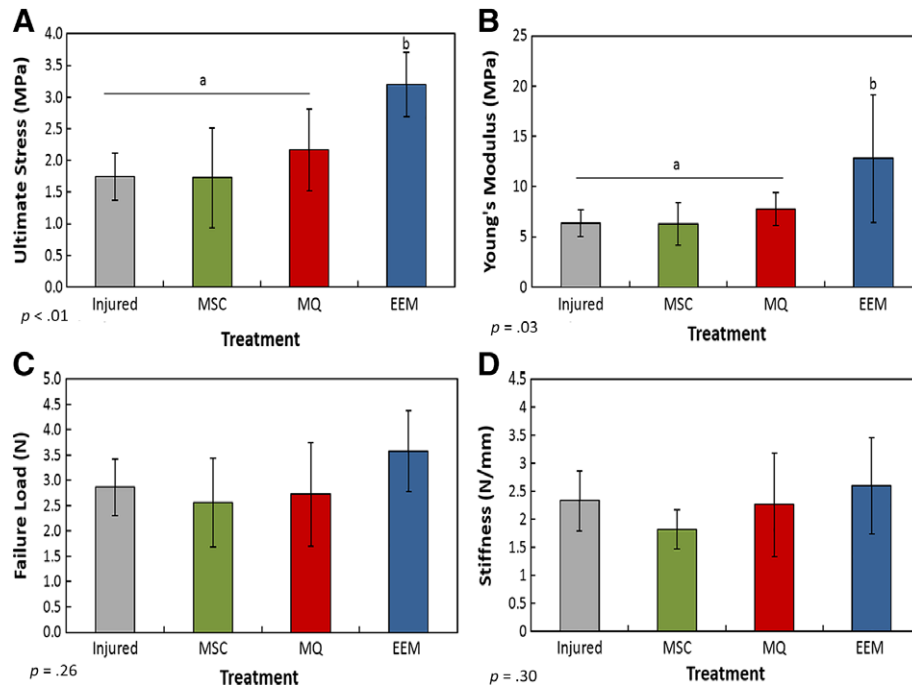
Figure 2. Mechanical results of the healing Achilles tendon after exosome-educated macrophage (EEM) treatment. Data indicate **(A)** ultimate stress, **(B)** Young's modulus, **(C)** failure load, and **(D)** stiffness of the Achilles tendons 14 days after injury after treatments with Hank's balanced saline solution ("injured"), mesenchymal stromal/stem cells, control macrophages, or EEMs. EEM treatment significantly improved (A) ultimate stress and (B) Young's modulus compared with all other treatments. No significance was found between (C) failure load and (D) stiffness. Bars without a common superscript within a graph indicate they are significantly different (results of Fisher's LSD post hoc pairwise analysis, $p < .05$). Results are expressed as mean $\pm$ SD.

injury, whereas the entire tendon ($p = .01$) was reduced in type I collagen content by day 14 (Fig. 4A, 4B). Type III collagen production (Fig. 4C, 4D) was not significantly altered with treatments, but the day 14 type I/type III collagen ratio (Fig. 4E) was reduced by the macrophages and EEMs ($p = .02$). Lastly, no significant differences at either time were noted with fractal analysis, a measure to quantify collagen organization (Fig. 4F).

Effect of EVs on Tendon Healing

To examine whether EVs treatment alone would be sufficient to improve tendon healing over EEM therapy, another group of animals were subjected to Achilles tendon injury, EV treatment, and tendon collection 14 days after injury to examine mechanical function, cellular factors and matrix production. At the concentrations used, treatment with EVs was not as effective at improving mechanical function when compared with EEM treatment (Supporting Information Fig. S3). With reference to the Achilles tendon cellular profile, M1 and M2 macrophages did not reach significance after treatment with EVs compared with the injured and EEM treatments (Supporting Information Fig. S4A, S4B). However, M1/M2 macrophage ratio was similarly reduced by the EEM and EV treatments (Supporting Information Fig. S4C). Interestingly, EV treatments significantly increased the number of endothelial cells 14 days after injury compared EEM treatment and injury only group (Supporting Information Fig. S4D). EVs also similarly reduced type I collagen within the healing tendon 14 days after injury when compared with EEM treatment (Supporting Information Fig. S4E). No treatment effects were observed with type III collagen, type I/III collagen ratio, or collagen organization (Supporting Information Fig. S4F–S4H).

DISCUSSION

To the best of our knowledge, this is the first study to test the potential benefits of in vitro generated, EV-educated macrophages (EEMs) on tendon healing. We previously reported that ligament injury resulted in a localized elevation of inflammatory M1 macrophages prior to scar formation and tissue compromise [36]. We also demonstrated that ligament and tendon healing could be improved using anti-inflammatory cytokines (e.g., IL-4, IL-1Ra) or MSC therapy to modulate macrophage phenotype [18, 20, 37–39]. In this study, we hypothesized that direct application of M2-like EEM macrophages would accelerate tendon healing by modulating tissue inflammation and endogenous macrophage phenotypes. Results herein support our hypothesis that EEM treatments significantly improve mechanical properties for tendon function as shown by ultimate stress and Young's modulus; reduce endogenous M1/M2 macrophage ratio indicating less inflammation; and increase the number of endothelial cells suggesting an acceleration of angiogenesis for more rapid healing. We were also able to detect the presence of implanted cells within the healing tendon by all treatment groups up to day 7 after injection. Lastly, treatment with EVs alone at the concentrations used to educate the macrophages were able to elicit a biological response but did not significantly improve mechanical function, further supporting the advantage of using EEMs in tendon healing and perhaps, in broader applications.

Macrophages are essential for the orchestration and promotion of proper wound healing as well as the resolution of inflammation in response to pathogenic challenge or tissue damage. The significance of macrophages during healing partially stems from earlier reports that total macrophage depletion, without taking
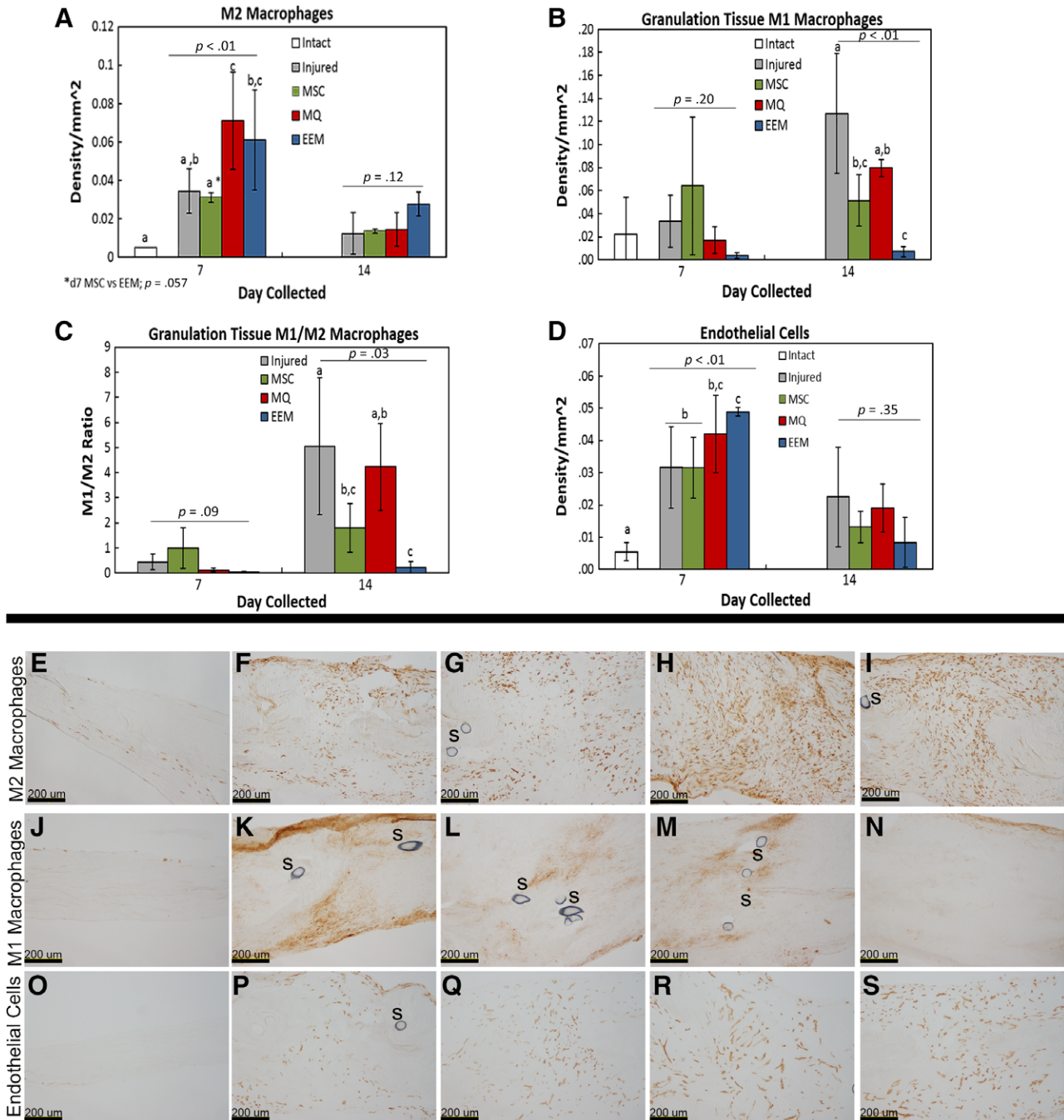
Figure 3. Immunohistochemistry results of the day 7 and 14 healing tendon. Graphs of **(A)** total M2 macrophages, **(B)** M1 macrophages localized to the granulation tissue, **(C)** M1/M2 macrophage ratio, and **(D)** endothelial cells within the healing Achilles tendon after treatment with Hank's balanced saline solution (injured), mesenchymal stromal/stem cells (MSCs), control macrophages (MQs), or exosome-educated macrophages (EEMs). Representative images of the **(E–I)** M2 macrophages, **(J–N)** M1 macrophages, **(O–S)** endothelial cells by the (E, J, O) intact, (F, P) day 7 injured, (G, Q) MSCs, (H, R) MQs, (I, S) EEM, and (K) day 14 injured, (L) MSC, (M) MQ, and (N) EEM. "S" indicates sutures within the tissue. Data are considered significantly different ($p < .05$) based on Fisher's LSD post hoc pairwise analysis. Within each bar graph, samples without a common superscript (a, b, c) are deemed significantly different. Values are expressed as mean cell numbers $\pm$ SD.

phenotype into account, is detrimental to wound re-epithelialization, angiogenesis, granulation tissue formation, and contraction [40–43]. Surprisingly, a paucity of studies has examined the effects of direct macrophage application on the regeneration process. One study administered activated macrophages to a cutaneous wound in guinea pigs, which resulted in a smaller wound area and improved integrity of barrier function measured by trans-

epidermal water loss [44]. Treatment of human ulcers with activated macrophages also promoted wound repair [45, 46]. Conversely, delivery of mouse M2 macrophages to skin wounds resulted in reduced re-epithelialization, persistent inflammation, and delayed wound healing [47, 48]. The inability to improve healing in mouse skin wounds may be attributed to the ratio of M1 to M2 macrophages present within the environment, but it
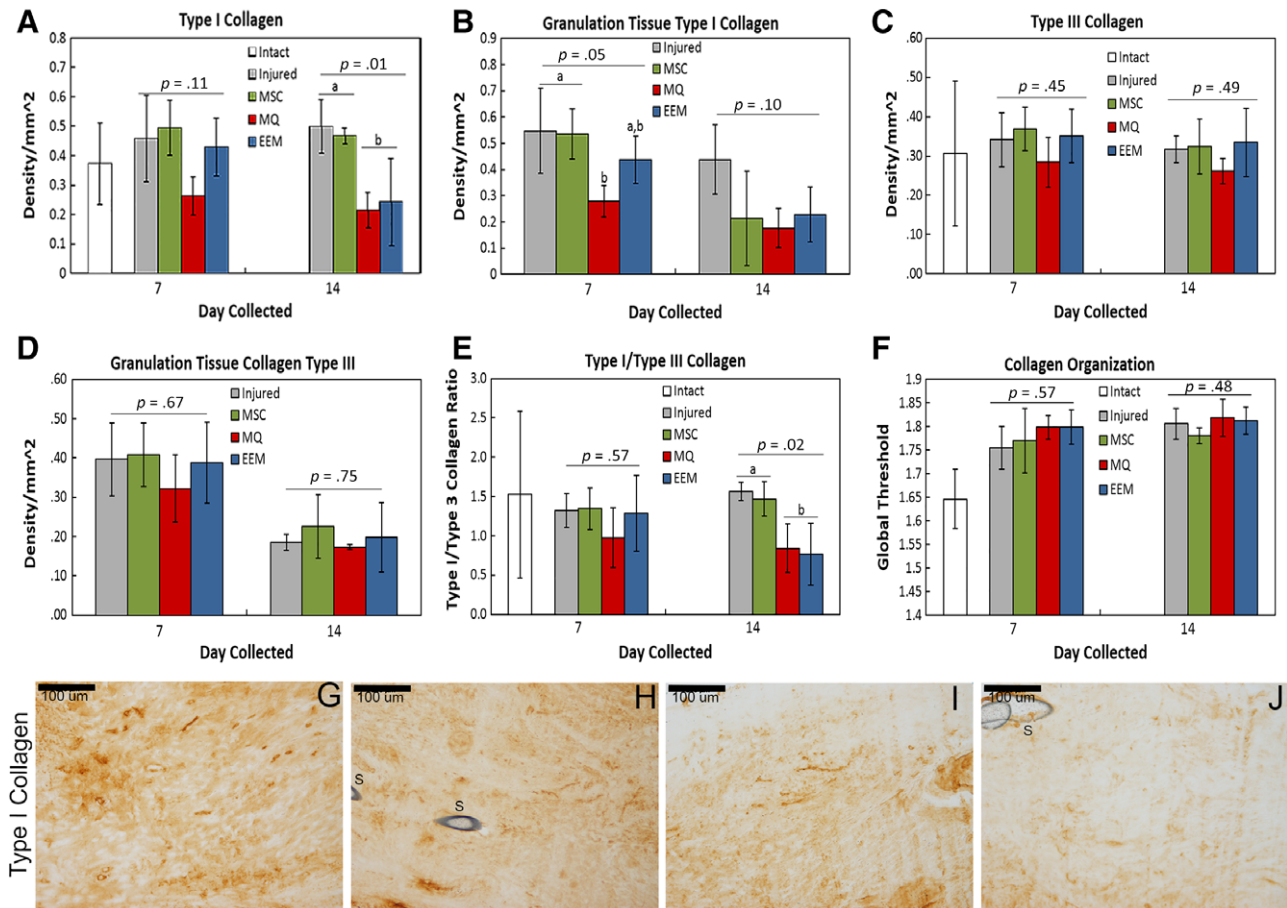
Figure 4. Immunohistochemistry results of extracellular matrix factors by day 7 and 14 healing tendon. Immunohistochemistry results showing the effects of mesenchymal stromal/stem cells (MSCs), control macrophages (MQs), and exosome-educated macrophages (EEMs) on **(A)** type I collagen throughout entire tendon, **(B)** type I collagen within the granulation tissue, **(C)** type III collagen throughout entire tendon, **(D)** type III collagen within the granulation tissue, **(E)** type I/type III collagen ratio, and **(F)** collagen organization. **(G–J):** Representative images of type I collagen by the day 14 Achilles tendon after (G) injured (control), (H) MSC, (I) MQ, or (J) EEM treatment. Data are considered significantly different ($p < .05$) based on Fisher's LSD post hoc pairwise analysis. Within each bar graph, samples without a common superscript (a, b) are deemed significantly different. Values are expressed as mean cell numbers $\pm$ SD.

is possible the number of M2 macrophages delivered was not sufficient to override an inflammatory environment and/or the delivered M2 macrophages switched to an M1 phenotype after placement into the inflammatory setting. Additional studies with these models could provide further insight into the discrepancies.

A number of studies have examined the in vitro effects of MSCs as well as adipose-derived stem cells (ASCs) on macrophage polarization [12, 23, 49–53]. MSCs have been shown to inhibit M1 markers such as TNF-α and iNOS, and promote M2 polarization [12, 23, 49, 50]. Recently, a comprehensive study examined the in vitro crosstalk between MSCs and macrophages across different activation stages. The authors reported that MSCs facilitated monocyte to macrophage transition, potentiated microbial responses, skewed naive macrophages to an M1 state, and attenuated already activated M1 macrophages while enhancing M2 activation [53]. Although the mechanisms controlling MSC induced macrophage polarization across different stages remain unclear, a few studies have identified some key factors. Nemeth et al. reported that LPS or TNF-α preconditioned MSCs can reprogram macrophages by releasing prostaglandin E2 (PGE2), which acts on the macrophages via the PGE receptors EP2

and EP4 [12]. Another study demonstrated changes in macrophage metabolic programs (glucose transporter 1 [GLUT] expression/ glucose uptake, indoleamine2,3-dioxygenase [IDO1] protein/activity, silent mating type information regulation 2 homolog 1 [SIRU-TIN1], AMP-activated protein kinase [AMPK], and rapamycin) after MSC coculture [53]. Additional studies are required to further elucidate the complexities of MSC modulated macrophage polarization.

In the current study, macrophages were educated with EVs, rather than direct coculture with MSCs, supporting a paracrine mediated mechanism by which MSCs polarize macrophages. Use of the MSC secretome (including soluble proteins, free nucleic acids, lipids, and EVs) to stimulate a paracrine mediated response has attracted considerable attention for its potential use in wound repair and regeneration. Earlier studies demonstrated that conditioned medium from MSCs exhibited therapeutic effects similar to or better than direct delivery of MSCs in some cardiac and lung injury models [54–56]. Although the specific MSC factors that induce wound healing are unknown, size fractionation and biophysical studies have partially attributed the biologically active components within the conditioned media as EVs. EVs (including apoptotic bodies, exosomes, and microvesicles) contain various

proteins, lipids, mRNAs, microRNAs, and tRNAs that are shuttled to the target cell to regulate gene expression and cell-to-cell communication. Studies examining the effects of EVs isolated from the conditioned media indicated the MSC derived EVs improved healing in various wound healing models, including critical-sized calvarial defects of an osteochondral femur injury [57–60].

We found EEM treatment accelerated tendon angiogenesis during healing. Studies on tendon healing have suggested that poor vascularity may prevent adequate tissue repair following trauma, leading to tendon weakening [61, 62]. There is also an increased incidence of tearing within the hypovascular regions of the Achilles, suggesting that pro-angiogenic therapies may promote tendon healing [61–63]. However, hypervascularity can also serve a detrimental role to tendon healing. For example, after injury, the highly organized tendon structure is disrupted after MMP-induced ECM degradation and vascular infiltration, resulting in a highly vascularized scar tissue with inferior biomechanical properties. In order to accelerate healing, the angiogenic response must therefore consist of a balance between early, rapid, and efficient development of capillaries after injury, followed by a quick regression to prevent functional compromise. Based on our work, EEM treatment supports the proposed angiogenic pattern to improve healing by increasing the number of endothelial cells during early healing and reducing them to lower levels prior to scar formation.

In our study, EVs isolated from MSC conditioned media were able to elicit a biological response as indicated by a reduced M1/M2 macrophage ratio and an increased number of endothelial cells 14 days after injury. However, direct treatment with EVs at the concentration tested did not improve tendon strength. The ability of EVs to enhance angiogenesis in other healing tissue models [64] has been documented, but this is the first study to the best of our knowledge to report it in healing tendon. These results suggest that optimized EVs may play a therapeutic role by limiting ischemic injury and/or stimulating angiogenesis to improve wound repair. However, for tendon repair to be successful, tendon mechanics must also improve with treatments. Future research (including dose response studies, timing of injections, etc.) is needed to understand the different mechanisms of EV and EEM-induced tendon healing.

Conclusion

We show for the first time that treatment with a novel type of myeloid cell resulted in superior tendon healing compared with all other treatments examined. The biological and functional improvements reported herein suggest EEM treatments accelerate the healing response. The use of EEM as a cell therapy to treat tissue injury has several attractive characteristics. EEMs are terminally differentiated and will not proliferate or differentiate into undesirable cell types, which is a concern with many stem cell types. For early treatment of traumatic injuries, EEMs generated from a patient's monocytes using off the shelf EVs can be obtained faster and with less processing than autologous MSCs. Despite promising results in numerous preclinical trials, MSCs have been not been consistently advantageous in clinical translation, and hence they have not become a standard of care for tendon healing [65–67]. Application of in vitro generated EEMs bypasses the indirect effect of MSCs on in situ macrophages. Altogether, results herein provide an alternative approach of using macrophages to improve tendon healing or other musculoskeletal injuries via modulation of tissue repair and inflammation.

Author Contributions

C.S.C.: manuscript writing, data analysis and interpretation, collection and/or assembly of data; A.E.B.C., J.A.K.: collection and/or assembly of data, data analysis and interpretation; U.C.: collection and/or assembly of data; G.S.B., M.A.H.: provision of study materials, final approval of manuscript; P.H.: concept and design, provision of study materials or patients, final approval of manuscript; R.V.: concept and design, manuscript writing, final approval of manuscript.

Disclosure of Potential Conflicts of Interest

The authors report no potential conflicts of interest.

Data Availability Statement

The data that support the findings of this study are available from the corresponding author upon reasonable request.

References

1 Mantovani A, Biswas SK, Galdiero MR et al. Macrophage plasticity and polarization in tissue repair and remodelling. J Pathol 2013; 229:176–185.

2 Murray PJ. Macrophage polarization. Annu Rev Physiol 2017;79:541–566.

3 Martinez FO, Helming L, Gordon S. Alternative activation of macrophages: An immunologic functional perspective. Annu Rev Immunol 2009; 27:451–483.

4 Godwin JW, Pinto AR, Rosenthal NA. Macrophages are required for adult salamander limb regeneration. Proc Natl Acad Sci USA 2013;110: 9415–9420.

5 Sindrilaru A, Peters T, Wieschalka S et al. An unrestrained proinflammatory M1 macrophage population induced by iron impairs wound healing in humans and mice. J Clin Invest 2011;121:985–997.

6 Benoit M, Desnues B, Mege JL. Macrophage polarization in bacterial infections. J Immunol 2008;181:3733–3739.

7 Weisberg SP, McCann D, Desai M et al. Obesity is associated with macrophage accumulation in adipose tissue. J Clin Investig 2003;112:1796–1808.

8 Eslani M, Putra I, Shen X et al. Cornea-derived mesenchymal stromal cells therapeutically modulate macrophage immunophenotype and angiogenic function. Stem Cells 2018;36(5): 775–784.

9 King SN, Hanson SE, Chen X et al. In vitro characterization of macrophage interaction with mesenchymal stromal cell-hyaluronan hydrogel

constructs. J Biomed Mater Res A 2014;102: 890–902.

10 Hanson SE, King SN, Kim J et al. The effect of mesenchymal stromal cell-hyaluronic acid hydrogel constructs on immunophenotype of macrophages. Tissue Eng Part A 2011;17:2463–2471.

11 Cantu DA, Hematti P, Kao WJ. Cell encapsulating biomaterial regulates mesenchymal stromal/stem cell differentiation and macrophage immunophenotype. Stem Cells Translational Medicine 2012;1:740–749.

12 Nemeth K, Leelahavanichkul A, Yuen PS et al. Bone marrow stromal cells attenuate sepsis via prostaglandin E(2)-dependent reprogramming of host macrophages to increase their interleukin-10 production. Nat Med 2009; 15:42–49.

13 Dayan V, Yannarelli G, Billia F et al. Mesenchymal stromal cells mediate a switch to alternatively activated monocytes/macrophages after acute myocardial infarction. Basic Res Cardiol 2011;106:1299–1310.

14 Gomez-Aristizabal A, Kim KP, Viswanathan S. A systematic study of the effect of different molecular weights of hyaluronic acid on mesenchymal stromal cell-mediated immunomodulation. PLoS One 2016;11:e0147868.

15 Yin F, Battiwalla M, Ito S et al. Bone marrow mesenchymal stromal cells to treat tissue damage in allogeneic stem cell transplant recipients: Correlation of biological markers with clinical responses. Stem Cells 2014;32:1278–1288.

16 Selleri S, Bifsha P, Civini S et al. Human mesenchymal stromal cell-secreted lactate induces M2-macrophage differentiation by metabolic reprogramming. Oncotarget 2016;7: 30193–30210.

17 da Silva CL, Goncalves R, Crapnell KB et al. A human stromal-based serum-free culture system supports the ex vivo expansion/maintenance of bone marrow and cord blood hematopoietic stem/progenitor cells. Exp Hematol 2005;33:828–835.

18 Aktas E, Chamberlain CS, Saether EE et al. Immune modulation with primed mesenchymal stem cells delivered via biodegradable scaffold to repair an Achilles tendon segmental defect. J Orthop Res 2016;35(2):269–280.

19 Saether EE, Chamberlain CS, Aktas E et al. Primed mesenchymal stem cells alter and improve rat medial collateral ligament healing. Stem Cell Rev 2016;12:42–53.

20 Chamberlain CS, Saether EE, Aktas E et al. Mesenchymal stem cell therapy on tendon/ligament healing. J Cytokine Biol 2017;2(1): 112–118.

21 Shen H, Kormpakis I, Havlioglu N et al. The effect of mesenchymal stromal cell sheets on the inflammatory stage of flexor tendon healing. Stem Cell Res Ther 2016;7:144.

22 Muir P, Hans EC, Racette M et al. Autologous bone marrow-derived mesenchymal stem cells modulate molecular markers of inflammation in dogs with cruciate ligament rupture. PLoS One 2016;11:e0159095.

23 Kim J, Hematti P. Mesenchymal stem cell-educated macrophages: A novel type of alternatively activated macrophages. Exp Hematol 2009;37:1445–1453.

24 Bouchlaka MN, Moffitt AB, Kim J et al. Human mesenchymal stem cell-educated macrophages are a distinct high IL-6-producing subset that confer protection in graft-versus-host-disease and radiation injury models. Biol Blood Marrow Transplant 2017;23:897–905.

25 Kourembanas S. Exosomes: Vehicles of intercellular signaling, biomarkers, and vectors of cell therapy. Annu Rev Physiol 2015; 77:13–27.

26 Anderson JD, Johansson HJ, Graham CS et al. Comprehensive proteomic analysis of mesenchymal stem cell exosomes reveals modulation of angiogenesis via nuclear factor-kappaB signaling. Stem Cells 2016;34:601–613.

27 Trivedi P, Hematti P. Derivation and immunological characterization of mesenchymal stromal cells from human embryonic stem cells. Exp Hematol 2008;36:350–359.

28 Dominici M, Le Blanc K, Mueller I et al. Minimal criteria for defining multipotent mesenchymal stromal cells. The International Society for Cellular Therapy position statement. Cytotherapy 2006;8:315–317.

29 Thery C, Amigorena S, Raposo G et al. Isolation and characterization of exosomes from cell culture supernatants and biological fluids. Curr Protoc Cell Biol 2006;30(1): 3.22.1 –3.22.29.

30 Chamberlain CS, Lee JS, Leiferman EM et al. Effects of BMP-12-releasing sutures on Achilles tendon healing. Tissue Eng Part A 2015;21:916–927.

31 Frisch KE, Marcu D, Baer GS et al. The influence of partial and full thickness tears on infraspinatus tendon strain patterns. J Biomech Eng 2014;136:051004.

32 Frisch KE, Duenwald-Kuehl SE, Kobayashi H et al. Quantification of collagen organization using fractal dimensions and Fourier transforms. Acta Histochem 2012;114:140–144.

33 Moisy F Boxcount. Fractal Dimension Using the 'Box-Counting' Method for 1D, 2D, and 3D sets. Available at www.mathworks.com.

34 Deng W, Chen W, Zhang Z et al. Mesenchymal stem cells promote CD206 expression and phagocytic activity of macrophages through IL-6 in systemic lupus erythematosus. Clin Immunol 2015;161:209–216.

35 Eslani M, Putra I, Shen X et al. Cornea-derived mesenchymal stromal cells therapeutically modulate macrophage immunophenotype and angiogenic function. Stem Cells 2018;36: 775–784.

36 Chamberlain CS, Crowley E, Vanderby R. The spatio-temporal dynamics of ligament healing. Wound Repair Regen 2009;17:206–215.

37 Chamberlain CS, Leiferman EM, Frisch KE et al. The influence of interleukin-4 on ligament healing. Wound Repair Regen 2011;19: 426–435.

38 Chamberlain CS, Leiferman EM, Frisch KE et al. Interleukin-1 receptor antagonist modulates inflammation and scarring after ligament injury. Connect Tissue Res 2014;55:177–186.

39 Chamberlain CS, Leiferman EM, Frisch KE et al. Interleukin expression after injury and the effects of interleukin-1 receptor antagonist. PLoS One 2013;8:e71631.

40 Chamberlain CS, Leiferman EM, Frisch KE et al. The influence of macrophage depletion on ligament healing. Connect Tissue Res 2011; 52:203–211.

41 Lucas T, Waisman A, Ranjan R et al. Differential roles of macrophages in diverse phases of skin repair. J Immunol 2010;184:3964–3977.

42 Mirza R, DiPietro LA, Koh TJ. Selective and specific macrophage ablation is detrimental to wound healing in mice. Am J Pathol 2009;175: 2454–2462.

43 Goren I, Allmann N, Yogev N et al. A transgenic mouse model of inducible macrophage depletion: Effects of diphtheria toxin-driven lysozyme M-specific cell lineage ablation on wound inflammatory, angiogenic, and contractive processes. Am J Pathol 2009;175:132–147.

44 Dachir S, Cohen M, Sahar R et al. Beneficial effects of activated macrophages on sulfur mustard-induced cutaneous burns, an in vivo experience. Cutan Ocul Toxicol 2014;33: 317–326.

45 Danon D, Madjar J, Edinov E et al. Treatment of human ulcers by application of macrophages prepared from a blood unit. Exp Gerontol 1997;32:633–641.

46 Zuloff-Shani A, Kachel E, Frenkel O et al. Macrophage suspensions prepared from a blood unit for treatment of refractory human ulcers. Transfus Apher Sci 2004;30:163–167.

47 Falanga V, Schrayer D, Cha J et al. Full-thickness wounding of the mouse tail as a model for delayed wound healing: Accelerated wound closure in Smad3 knock-out mice. Wound Repair Regen 2004;12:320–326.

48 Jetten N, Roumans N, Gijbels MJ et al. Wound administration of M2-polarized macrophages does not improve murine cutaneous healing responses. PLoS One 2014;9:e102994.

49 Abumaree MH, Al Jumah MA, Kalionis B et al. Human placental mesenchymal stem cells (pMSCs) play a role as immune suppressive cells by shifting macrophage differentiation from inflammatory M1 to anti-inflammatory M2 macrophages. Stem Cell Rev 2013;9:620–641.

50 Maggini J, Mirkin G, Bognanni I et al. Mouse bone marrow-derived mesenchymal stromal cells turn activated macrophages into a regulatory-like profile. PLoS One 2010;5: e9252.

51 Hu Y, Qin C, Zheng G et al. Mesenchymal stem cell-educated macrophages ameliorate LPS-induced systemic response. Mediators Inflamm 2016;2016:3735452.

52 Torihashi S, Ho M, Kawakubo Y et al. Acute and temporal expression of tumor necrosis factor (TNF)-alpha-stimulated gene 6 product, TSG6, in mesenchymal stem cells creates microenvironments required for their successful transplantation into muscle tissue. J Biol Chem 2015;290:22771–22781.

53 Vasandan AB, Jahnavi S, Shashank C et al. Human mesenchymal stem cells program macrophage plasticity by altering their metabolic status via a PGE2-dependent mechanism. Sci Rep 2016;6:38308.

54 Gnecchi M, He H, Liang OD et al. Paracrine action accounts for marked protection of ischemic heart by Akt-modified mesenchymal stem cells. Nat Med 2005;11:367–368.

55 Goolaerts A, Pellan-Randrianarison N, Larghero J et al. Conditioned media from mesenchymal stromal cells restore sodium transport and preserve epithelial permeability in an in vitro model of acute alveolar injury. Am J Physiol Lung Cell Mol Physiol 2014;306:L975–L985.

56 Aslam M, Baveja R, Liang OD et al. Bone marrow stromal cells attenuate lung injury in a murine model of neonatal chronic lung disease. Am J Respir Crit Care Med 2009;180: 1122–1130.

57 Qi X, Zhang J, Yuan H et al. Exosomes secreted by human-induced pluripotent stem cell-derived mesenchymal stem cells repair critical-sized bone defects through enhanced angiogenesis and osteogenesis in osteoporotic rats. Int J Biol Sci 2016;12:836–849.

58 Zhang S, Chu WC, Lai RC et al. Exosomes derived from human embryonic mesenchymal stem cells promote osteochondral regeneration. Osteoarthr Cartil 2016;24:2135–2140.

59 Bruno S, Grange C, Deregibus MC et al. Mesenchymal stem cell-derived microvesicles protect against acute tubular injury. J Am Soc Nephrol 2009;20:1053–1067.

60 Lai RC, Arslan F, Lee MM et al. Exosome secreted by MSC reduces myocardial ischemia/reperfusion injury. Stem Cell Res 2010;4:214–222.

61 Ahmed IM, Lagopoulos M, McConnell P et al. Blood supply of the Achilles tendon. J Orthop Res 1998;16:591–596.

62 Galatz LM, Gerstenfeld L, Heber-Katz E et al. Tendon regeneration and scar formation: The concept of scarless healing. J Orthop Res 2015;33:823–831.

63 Akhavani MA, Sivakumar B, Paleolog EM et al. Angiogenesis and plastic surgery. J Plast Reconstr Aesthet Surg 2008;61:1425–1437.

64 Kholia S, Ranghino A, Garnieri P et al. Extracellular vesicles as new players in angiogenesis. Vascul Pharmacol 2016;86:64–70.

65 Battiwalla M, Hematti P. Mesenchymal stem cells in hematopoietic stem cell transplantation. Cytotherapy 2009;11:503–515.

66 Leong DJ, Sun HB. Mesenchymal stem cells in tendon repair and regeneration: Basic understanding and translational challenges. Ann N Y Acad Sci 2016;1383:88–96.

67 Depres-Tremblay G, Chevrier A, Snow M et al. Rotator cuff repair: A review of surgical techniques, animal models, and new technologies under development. J Shoulder Elbow Surg 2016;25:2078–2085.

See www.StemCells.com for supporting information available online.